Korean J. Chem. Eng., 36(8), 1321-1327 (2019)
DOI: 10.1007/s11814-019-0310-2

pISSN: 0256-1115
eISSN: 1975-7220

Selective separation of copper and zinc and regeneration of polymer from electroplating effluent using shear induced dissociation coupling with ultrafiltration

Shu-Yun Tang and Yun-Ren Qiu†

School of Chemistry and Chemical Engineering, Central South University, Changsha 410083, China
(*Received 2 February 2019 • accepted 25 May 2019*)

Abstract−Shear-induced dissociation coupling with ultrafiltration (SID-UF) was used to remove and separate copper and zinc from both simulative effluent and real electroplating effluent using polyacrylate sodium (PAAS) as complexant. The effects of pH and the mass ratio of polymer on metal ions (P/M) on the removal of copper and zinc were investigated in the ultrafiltration tests, and the optimum pH and P/M were 7.0 and 25, respectively. The shear rate distributions on the membrane surface at various rotating speeds were simulated by CFD software. The shear stabilities of the polymer-metal complexes studied at various pHs indicated that the complexes would dissociate when the shear rate exceeded the critical shear rates (γ_c), and the order of critical shear rate was PAA-Zn>PAA-Cu at the same pH. The contrast between these two complexes shear stabilities was used to separate copper and zinc and recovery complexant from electroplating effluent by SID-UF. The results show that copper and zinc can be separated at $1.06\times10^5\ s^{-1}<\gamma<1.58\times10^5\ s^{-1}$ at pH 7.0, and PAAS can also be regenerated at $\gamma>1.58\times10^5\ s^{-1}$. Compared to conventional complexation-ultrafiltration, SID-UF is a green and efficient method for the separation of metals and the regeneration of complexant.

Keywords: Selective Separation, Shear Induced Dissociation, Ultrafiltration, Shear Stability, Electroplating Effluent

INTRODUCTION

Wastewater containing heavy metal ions is a major environmental concern, as large amounts of wastewater discharged from metal plating industry contain heavy metal ions, for example, copper and zinc, which are classified as toxic elements and serious environmental contaminants [1,2]. It is essential to separate and recover these heavy metals from the industrial effluents before discharging into nature, which not only can eliminate heavy metal hazard, but also bring economic benefits. Numerous methods are employed to remove metal ions from wastewater, such as precipitation, adsorption, membrane filtration and ion exchange [3]. Chemical precipitation is one of the most popular and economical methods due to its simplicity [4]. However, the wastewater treatment ability of this method in some of the heavy metal ions is quite limited, especially for low concentrations. Generally, the concentration of the heavy metals in the effluents still remains on the level of mg/L after several precipitations, and the residual heavy metals are difficult to remove by chemical precipitation [5,6]. Ion-exchange, adsorption and membrane filtration have proven to be effective routines for removing the low concentration metal ions, but large-scale industrial applications are difficult to achieve due to their high operational cost, low reuse and complicated conditions [7-9]. In addition, the coexistence of various metal ions in wastewater further makes them harder to treat by traditional methods, especially for the selective separation of metal ions. Therefore, it is imperative to find a green and efficient technology to removal heavy metal from wastewater, especially for the separation and recovery of the several heavy metals.

Shear-induced dissociation coupling with ultrafiltration (SID-UF), a novel technology, has been used for the removal and separation of the several metal ions from wastewater. SID-UF mainly includes two processes, using water soluble polymer to bind heavy metals and the polymer-metal complexes can be rejected by ultrafiltration membrane, and then metal ions can be separated and recovered by SID-UF according to the difference of critical shear rate of polymer-metal complexes. Similar to conventional complexation-ultrafiltration, macromolecular polymer is used to bind the heavy metals to form complexes, and the aqueous solution is treated by ultrafiltration to retain the complexes, while the free heavy metals permeate through the membrane [10-12]. The complexation-ultrafiltration shows low energy and simple conditions requirements [13-15]. However, for conventional complexation-ultrafiltration, the recovery of the metal-loaded polymers is always achieved by acidification, and followed by the addition of alkali. The selective separation of various heavy metals is very difficult, despite it could be fulfilled by looking for different polymers or incorporating other functional groups to the polymer [16,17] because the preparation or functionalization of polymers is always complicated and the cost is high. SID-UF differs from conventional complexation-ultrafiltration, the selective separation of metal ions and the recovery of the metal-loaded complexants are implemented by providing suitable shear rate through dynamic shear enhanced membrane module, which can ensure the dissociation of polymer-metal complexes and then separate or concentrate complexants and metal ions by ultrafiltration. This process avoids the use of a large amount of acid and alkali. Meanwhile, the regenerated polymer can be directly used as complexing agent. Rotating disk membrane is one of the dynamic shear enhanced membrane modules, which generates shear rate in

†To whom correspondence should be addressed.
E-mail: csu_tian@csu.edu.cn

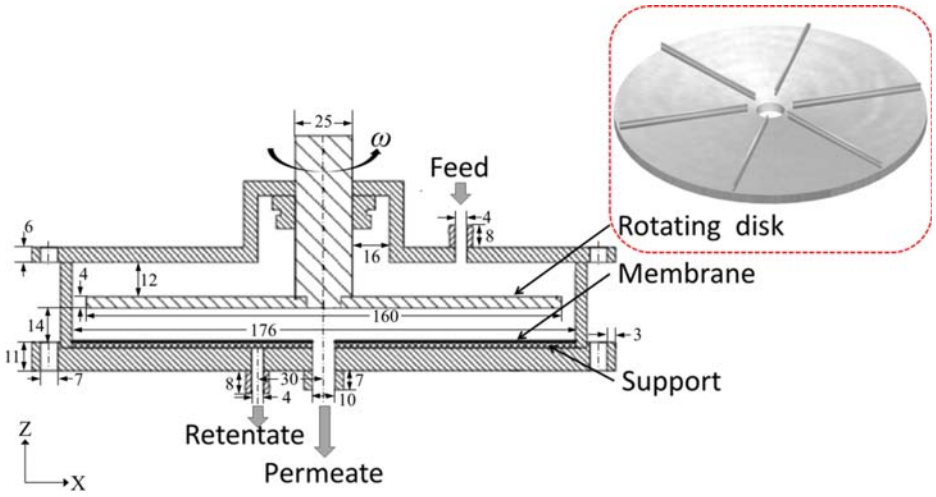

Fig. 1. Schematic diagram of the RDM system.

the filtration. Rotating disk membrane has been efficiently applied in many fields, such as the harvesting of microalgae [18], the removal of fine particles from seawater [19] and the concentration of leaf protein [20,21]. In our studies, the rotating disk membrane is used to generate shear field to study the shear stabilities of complexes for the selective separation of the heavy metals and the recovery of polymer from aqueous solution. The critical shear rates of polymer-metal complexes γ_c vary from metal to metal at a certain pH, and can be used to selective separate of some heavy metal ions and the recovery of complexant from aqueous solution [22-25].

In this work, SID-UF was used to remove and separate copper and zinc ions from both simulative effluent and real electroplating effluent (after precipitation) using rotating disk membrane. The influence of rotating speed on the shear rate distributions on the membrane surface was simulated by CFD software, and the complexes γ_c were obtained at different pHs, respectively. Further, SID-UF was used to separate copper and zinc ions and recover PAAS according to the difference of shear stabilities of these two complexes.

MATERIAL AND METHOD

1. Reagents, Membrane and Apparatus

The metal plating wastewater samples were obtained from a zinc metal-plating facility in Changsha, China. The chemical and physical parameters of the electroplating effluent used in our study are listed in Table 1. The samples were analyzed for pH, metal concentrations (Zn (II), Cu (II), Cr (III), Fe (III)), and color. Before the experiments were performed, the electroplating effluent was filtered using microfiltration membrane (membrane pore size 0.8 μm, supplied by Tianjin Jinteng Laboratory Equipment Co, Ltd.) to remove the insoluble matters. As for the simulative effluent, Cu (II) chloride dehydrate ($CuCl_2 \cdot 2H_2O$) and Zn (II) chloride dehydrate ($ZnCl_2 \cdot 2H_2O$) were used as copper and zinc sources, respectively, for laboratory aqueous solution. The concentration of copper and zinc ions was 10 mg/L unless special illustration. The molecular weight of the complexant polyacrylate sodium (PAAS) is 250 kDa. Either NaOH (0.1 M) or HCl (0.1 M) served to adjust wastewater pH. Hyperpure water was used in the experiments. The concentrations of different metal ions and complexants were analyzed by inductively coupled plasma optical emission spectrometry (ICP-OES) and total organic carbon (TOC), respectively. The complexants were pretreated using diafiltration to remove the small polymers [14].

Table 1. Some physicochemical characteristics of the electroplating effluent before/after precipitation

Parameter	Original effluent	After precipitation
pH	2.8±0.2	7.5
Zn^{2+} (mg/L)	209.2±3.1	78.2
Cu^{2+} (mg/L)	23.6±1.0	13.5
Cr^{3+} (mg/L)	49.4±1.2	<0.1
Fe^{3+} (mg/L)	14.9±0.1	<0.1
Color	Yellow	Clear

Filtration tests were performed in the experimental set-up described in our previous work [22]. A principal scheme of the RDM used in our laboratory is shown in Fig. 1. The fluid flow directions are represented by the coordinates. The module is made up with a metal rotating disk with six vanes in the filtration chamber near the flat membrane (30 kDa). The distance between flat membrane and disk is 14 mm and the radius of disk and cylindrical housing are 80 mm and 88 mm, respectively. Vanes are distributed uniformly at the disk surface, which height and width are 4 and 1 mm, respectively. The motor with the axial connection can increase the rotating speed to 3,000 rpm.

2. Full Recycle Tests

The UF tests were carried out in full recycle process. The permeate and the retentate were returned to the raw material tank to keep the concentration of feed constant. The metal ions absolutely reacted with complexants for about two hours, and the obtained materials were filled into the filtration chamber by peristaltic pump. The initial peripheral pressure was 0.01 MPa. Five minutes after beginning of each rotating speed, the permeates were collected for 30 s and further analyzed for determining metal ions, PAAS concentrations and permeate volume. All the experiments were car-

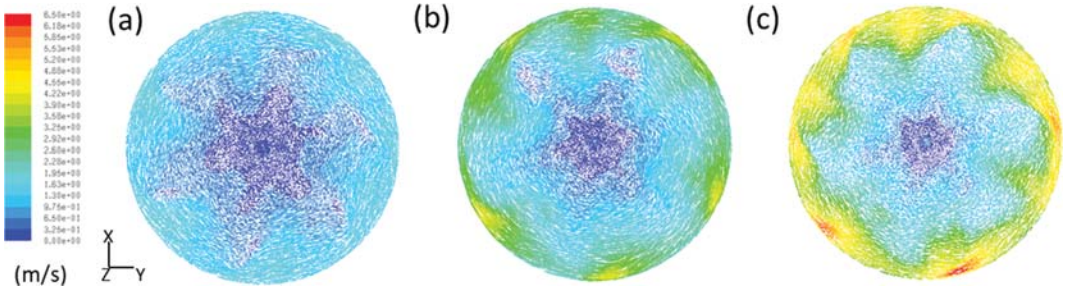

Fig. 2. Simulated fluid velocity distribution on the membrane surface at different rotating speeds, (a) N=1,000 rpm, (b) N=2,000 rpm, (c) N= 3,000 rpm (inlet velocity, 0.5 m/s).

ried out at 25 °C.

3. Diafiltration Tests

In diafiltration tests, the permeate stream is not returned and an amount of hyperpure water (at the appropriate pH depending on the type of test) is added to the raw material tank simultaneously to maintain the volume of feed. Samples are collected in permeate at every unit of volume of make-up water. Each tests run is stopped when the permeate concentration is constant. After the full recycle test and the diafiltration test, the device is washed by hyperpure water about quarter of an hour at rest. All the experiments were carried out at 25 °C.

4. Numerical Simulation Methods

The distributions of velocity and the distributions of shear rate were simulated using the computational fluid dynamics software (CFD) of Gambit 2.4 and Fluent 6.3. To prepare for the simulation, the Gambit software was used to build model and mesh (3-dimensional unstructured T-grid) of the filtration chamber, and set boundary conditions (one velocity inlet and one outflow). The mesh used in the simulations contained approximately 590,000 elements. Fluent software was used to carry out a series of simulations. Reynolds stress turbulence model and SIMPLE algorithm were used. Moving reference frame method was used to simulate the disk rotating and no slip condition was set for walls. The convergence criteria were all of the residuals below 10^{-3}.

RESULTS AND DISCUSSION

1. The Radial Distribution of Shear Rate on the Membrane Surface

Simulating the velocity distribution and the shear stress using CFD software is a highly effective, economical and time-saving way that can give insight into the shear stabilities of complexes by discussing velocity distributions and shear rate distributions [26]. Fig. 2 shows simulated fluid velocity distribution on the membrane surface at different rotating speeds. The inlet fluid velocity is 0.5 m/s. The velocity on the membrane surface at a fixed position increases with the elevated rotating speeds. The radial velocity also increases when the radius grows. In addition, the velocity is relatively high in the regions near the vanes. The shear rate distribution can be estimated when the velocity field is simulated.

Fig. 3 compares the theoretically calculated and the simulated shear rate distributions on the membrane surface. The shear rate distributions could be calculated based on the previous studies [22, 27]. Obviously, the simulated values are highly in accordance with

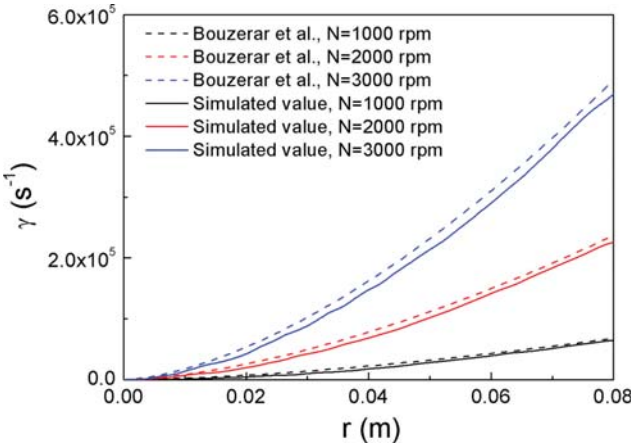

Fig. 3. Distribution of the shear rate on the membrane surface at different rotating speeds (initial pressure, 0.01 MPa; inlet velocity, 0.5 m/s).

the calculated results under similar conditions. Thus, we can infer that the simulated way used in our study is reliable. The shear rate tends to increase with the rotating speed in Fig. 3, which is due to the large velocity gradient between the fixed membrane and the rotating disk [28]. In addition, the shear rate also increases when the radius grows at the same speed condition, which is similar to the velocity distribution in radial direction. In the simulated results, the lowest shear rate is observed in the center, and the shear rate

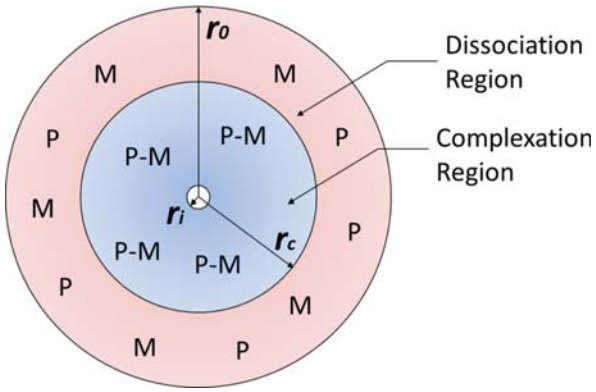

Fig. 4. The distribution of the form of metals on the membrane surface in the shear field.

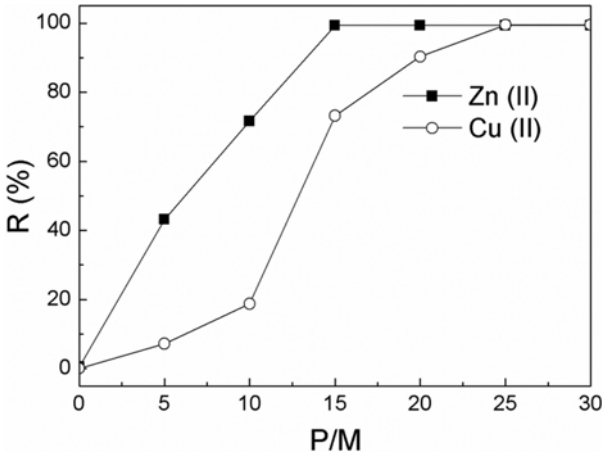

Fig. 5. Effect of P/M on the rejections of Zn (II) and Cu (II) in mixture solution (pH 7.0; copper concentrations, 10 mg L^{-1}; zinc concentrations, 10 mg L^{-1}; rotating speed, 0 rpm).

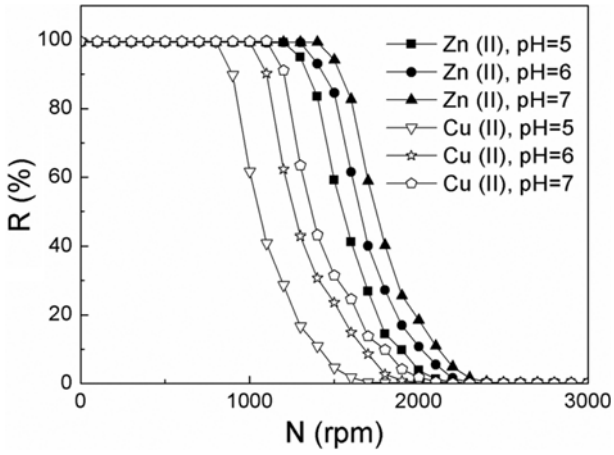

Fig. 6. Effect of rotating speed on the rejection of zinc (II) and copper (II) in mixture solution at different pHs (P/M=30; copper concentrations, 10 mg L^{-1}; zinc concentrations, 10 mg L^{-1}).

sharply increases when the radius grows. The shear rate differences could induce the polymer-metal dissociation at the high shear rate and the ideal models of metals distribution are depicted in Fig. 4, where P-M represents polymer-metal complex. P and M represent polymer and metal ions after the polymer-metal complex dissociation, respectively. The free metal ions mainly exist in the dissociation region and the polymer-metal complexes exist in the complexation region. The critical shear rate of complexes γ_c relies on the metal species at a certain pH [22-25]. Therefore, the removal and the separation of the mixed metal ions can be achieved by SID-UF due to the different critical shear rates. The critical radius r_c is the radius position of complexes beginning to dissociate.

2. Selection of P/M and pH

The influence of P/M on the removal of zinc and copper in mixture solutions at pH 7.0 is presented in Fig. 5. When the P/M< 10, the rejection of copper is growing slowly and less than 17.8%, while the rejection of zinc is rapidly growing to above 71.6%. When P/M exceeds 15, the rejection of zinc always maintains to ~99.6%, and the rejection of copper increases to 99.5%. When P/M exceeds 25, the rejections of the copper and zinc hold steady. These results can be explained as follows: the limited deprotonated complexant first bonds with zinc ions to form complex due to the better complexing capabilities [29,30] when the amount of PAAS is minor enough, while with the increasing amount of PAAS, almost all zinc ions have bonded with complexant, and the excessive complexants bond with copper ions, which results in the increasing of the rejection of copper.

As one of the important factors of the rejection, the effects of pH on the zinc and copper rejections were studied [22,23]. The rejection of zinc is very low at pH<3.0 and increases significantly at pH>3.0, and can reach to ~100% at pH from 7.0 to 8.0. Similarly, the rejection of copper is also very low at pH<4.0. When the pH> 4.0, especially ranging from 5.5 to 7.0, the rejection of copper is up to about 100%. At relatively low pH, the affinities of complexing agent towards heavy metal ions tended to reduce because of the high hydrogen ion concentration. The complexant is in the deprotonation state at high pH, which is beneficial for the formation of polymer-metal complexes. However, it is possible that heavy metal ions form hydroxide precipitation at alkaline conditions leading to the membrane fouling. To remove zinc and copper simultaneously and effectively, pH 7.0 was selected as the optimal pH.

3. The Shear Stability of PAA-Zn Complex and PAA-Cu Complex in Mixture Solutions

The shear stabilities of the polymer-metals in the shear field are directly associated with their separation. To compare the stabilities of the both PAA-Cu and PAA-Zn, the rejections of the polymer-metals at different rotating speeds have been investigated in Fig. 6. To ensure the heavy metals complexed completely, the effects of rotating speeds on the rejections of zinc and copper were investigated using 600 mg/L PAAS. It can be seen that the metal rejections reached ~100% at zero rotary speed (N=0rpm). As shown in Fig. 6, the rejection rate initially remains constant and then rapidly reduces with the improvement of speed, when the rotating speed (N) exceeds critical rotating speed (N_c). Interestingly, N_c of PAA-Cu complex are 890, 1,020 and 1,170 rpm at pH 5.0, 6.0 and 7.0, respectively, while those of PAA-Zn complex are 1,280, 1,390 and 1,460 rpm, respectively. In the previous studies, the complexant could hold steady at 0-3,000 rpm [22]. Therefore, the cause of the rejection decline could be attributed to the cleavage of coordination bonds PAA-Zn and PAA-Cu at the high shear rates.

According the previous study [22], the velocity factor k of the six rectangular blades in this module is 0.796, and r_c could be calculated by Eq. (1).

$$r_c^4+\frac{364P_0}{\rho k^2N^2}r_c^2-\frac{C_0-C_p}{C_0-C_s}\left(r_m^4+\frac{364P_0}{\rho k^2N^2}r_m^2\right)-\frac{C_p-C_s}{C_0-C_s}\left(r_0^4+\frac{364P_0}{\rho k^2N^2}r_0^2\right)=0 \quad (1)$$

where r_m and r_0 are the membrane outside and inside radius (m), respectively. P_0 is the center pressure (kPa). ρ is the fluid density (kg m^{-3}). C_0, C_p and C_s are the metal ion concentrations in permeate under static state operation, permeate and feed stream, respectively. The r_c at various rotating speeds are illustrated in Fig. 7. When the rotating speed exceeds the N_c, the r_c significantly decreases with the rising N_c. The γ_c of a complex at certain pH is constant, while the γ increases with the speed. With the speed increasing,

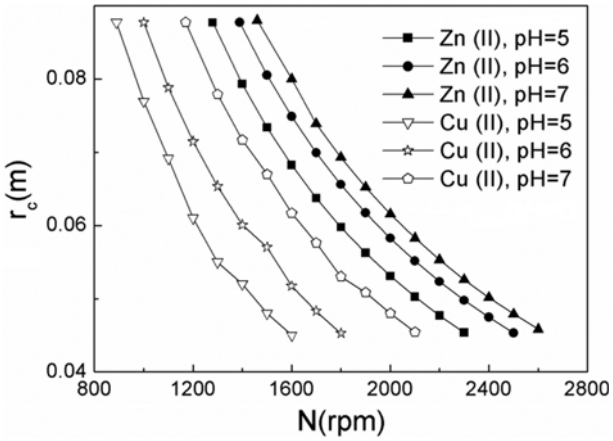

Fig. 7. The relationships between the critical radius of PAA-Zn and PAA-Cu complexes and the rotating speed at different pHs.

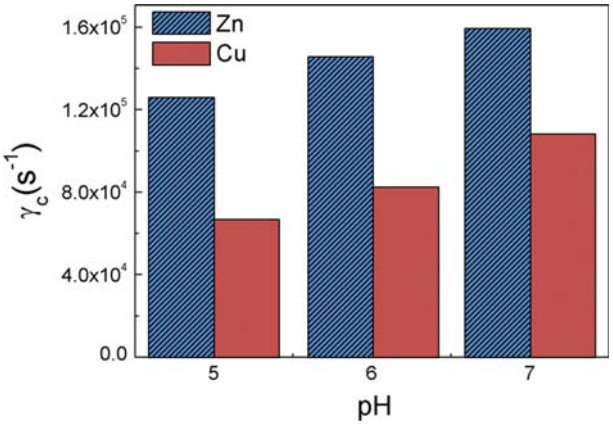

Fig. 8. Critical shear rates of PAA-Zn and PAA-Cu complexes at different pHs.

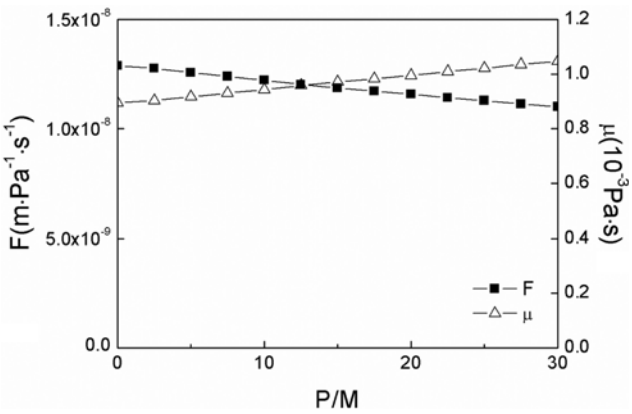

Fig. 9. Effect of P/M on the viscosities and the permeate flux of unit pressure (pH 7.0; copper concentrations, 10 mg L^{-1}; zinc concentrations, 10 mg L^{-1}; rotating speed, 500 rpm).

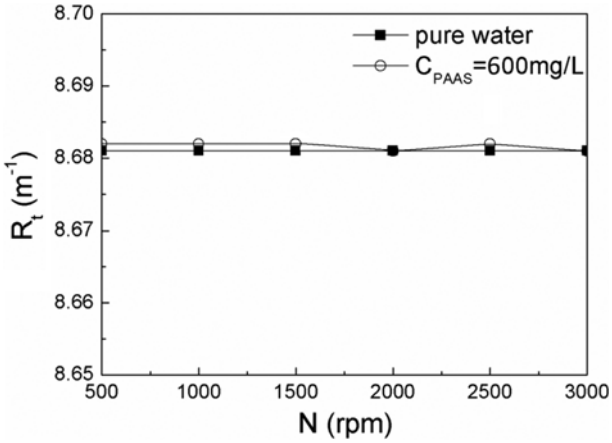

Fig. 10. The variability of the total resistance of pure ultrapure water and 600 mg/L PAAS with the rotating speed.

the dissociation region is extended to the membrane center, leading to the critical radius decrease [24].

The γ_c of the PAA-Zn and PAA-Cu can be calculated according to the r_c [27]. As shown in Fig. 8, the γ_c of PAA-Cu complex are 6.5×10^4, 8.0×10^4 and 1.06×10^5 s^{-1} at pH 5.0, 6.0 and 7.0, respectively, and those of PAA-Zn complex are 1.25×10^5, 1.45×10^5 and 1.58×10^5 s^{-1}, respectively. It can be observed that γ_c of PAA-Metal complexes increase with the increase of pHs. This is related to the deprotonation degree of PAAS at different pH [31,32]. Clearly, the stabilities of the complexes depend on the speeds and pH, and $\gamma_{c(PAA\text{-}Zn)}>\gamma_{c(PAA\text{-}Cu)}$ at the same pH.

4. Effect of Rotating Speed on the Resistance

For further discussion of the effects of rotating speeds on the permeate flux, the samples were collected in permeate in 30 s after the beginning of each rotating speed decrement at the range from 500 rpm to 3,000 rpm. Based on the Darcy's law, we know that the total resistance $R_t=\Delta P/(J\mu)=1/(F\mu)$, where the permeate flux of unit pressure F and the dynamic viscosity μ can be obtained by experiments [22], The effects of P/M on μ and F are shown in Fig. 9. With the increase of the P/M, μ is growing slowing and F is falling slightly. And $R_t=R_m+R_f+R_c$, where R_m is the membrane intrinsic resistance, can be determined by pure water experiment, R_f is the membrane fouling and R_c is the concentration polarization resistance [22]. The effect of N on R_t of hyperpure water and 600 mg/L PAAS are shown in Fig. 10. The R_t of 600 mg/L PAAS keep stable without significant fluctuation in 500-3,000 rpm, and the results are similar to that of hyperpure water, denoting that $R_t=R_m$, and the concentration polarization and membrane fouling are ignorable at high shear rate and the low concentration of solute [13,33].

5. Determination of Selective Separation Coefficient

Selective separation coefficient ($\beta_{Cu/Zn}$) reflects the separated degree of copper and zinc, which could be defined by the following equation [34]:

$$\beta_{Cu/Zn}=\frac{1-R_{Cu}}{1-R_{Zn}} \tag{2}$$

where R_{Cu} and R_{Zn} are the rejections of copper and zinc, respectively.

The selective separation and the regeneration experiments were carried out at P/M=30 and different pHs. The effect of the N on the $\beta_{Cu/Zn}$ is shown in Fig. 11. It is easy to see that $\beta_{Cu/Zn}$ first keeps relatively stable when the N is lower than the N_c of PAA-Cu, and

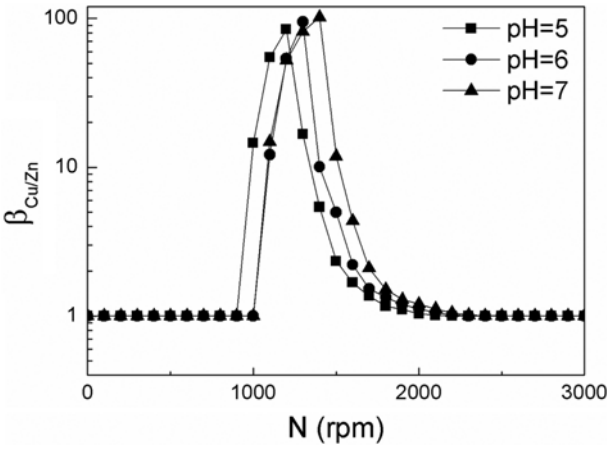

Fig. 11. Effect of rotating speeds on selective separation coefficient $\beta_{Cu/Zn}$ at different pHs.

then it shows a remarkable increase, further followed by a significant drop. This could be interpreted as when $\gamma<\gamma_{c(PAA\text{-}Cu)}$, both of the PAA-Cu and PAA-Zn complexes remain stable. When the N exceeds the N_c of PAA-Cu complex, the γ is higher than the γ_c of PAA-Cu complex, which results in the PAA-Cu complex dissociation and the decrease of R_{Cu}, while PAA-Zn complex remains stable, so R_{Zn} keeps constant. Therefore, $\beta_{Cu/Zn}$ shows an enlargement trend. When $\gamma>\gamma_{c(PAA\text{-}Zn)}$, the bond of PAA-Zn also begins to break, resulting to the decline of R_{Zn} and $\beta_{Cu/Zn}$. Thus, this enables high separation rates of copper and zinc to be achieved by selecting the appropriate rotating speed, at which the generated shear rate is between $\gamma_{c(PAA\text{-}Cu)}$ and $\gamma_{c(PAA\text{-}Zn)}$. The greatest selection separation coefficients are 84.4, 94.7 and 101.9 at pH 5.0 1,200 rpm, pH 6.0 1,300 rpm and pH 7.0 1,400 rpm, respectively.

6. Selective Separation of Copper and Zinc and Recovery of PAAS from Simulated Wastewater

The simulated wastewater was prepared based the concentrations of copper (10 mg/L), zinc (10 mg/L) and PAAS (500 mg/L). The selective separation and the regeneration experiments were

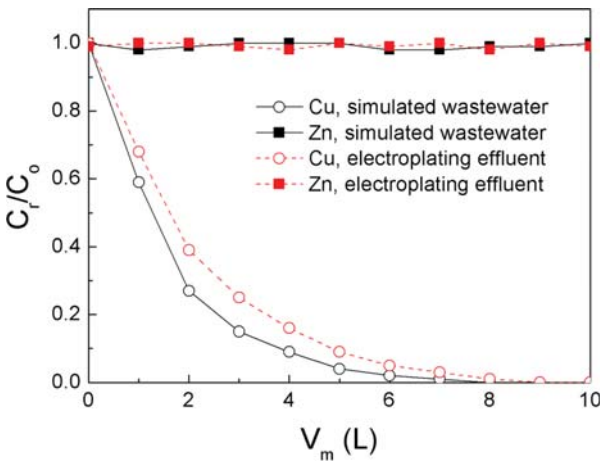

Fig. 12. The variations of the concentration ratio of copper and zinc in retentate to original solution with the volume of make-up water at 1,400 rpm.

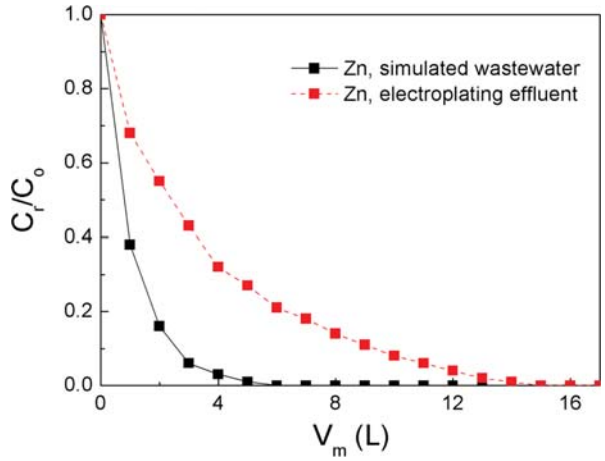

Fig. 13. The variations of the concentration ratio of zinc in retentate to original solution with the volume of make-up water at 2,400 rpm.

carried out at pH 7.0. In rotating disk diafiltration experiments, an amount of hyperpure water is added to the raw material tank simultaneously to maintain the volume of feed. The rotating speed is adjusted to 1,400 rpm for diafiltration experiments to separate copper and zinc. The PAA-Cu complex is easily dissociated at this shear rate, and the copper ions penetrate the ultrafiltration membrane into permeate. Fig. 12 shows the variations of the concentration ratios (C_r/C_o) of heavy metals in retentate to original solution with the make-up water volume (V_m) at 1,400 rpm.

When the separation of copper is complete, the test of separation of zinc and PAAS can be carried out. The regeneration of PAAS can be achieved by SID-UF at 2,400 rpm. At 2,400 rpm the γ reaches to $3.86\times10^5\ s^{-1}$, which exceeds the γ_c of PAA-Zn complex. Therefore, PAA-Zn complex dissociates and the zinc ions are collected in permeate, while the PAAS still remains in the retentate, as shown in Fig. 13. It is shown that the zinc is collected in permeate completely when V_m reaches 6.0 L. Then the diafiltration experiment is carried out without any water to the feed tank, and the regenerated PAAS is obtained about 20 min later.

7. Selective Separation of Copper and Zinc and Recovery of PAAS from Electroplating Effluent

To further explore the feasibility of the SID-UF routine in practical application, the real electroplating effluent mainly containing copper and zinc was selected to classify the copper and zinc at the same conditions. The ferrum, chromium, partial copper and partial zinc in electroplating effluent were initially precipitated by chemical precipitation methods (adjusting the pH to 7.5) before the SID-UF experiments [35,36]. The precipitating process is very important, which can eliminate the effects of the other impurities such as ferrum and chromium. After precipitation, the residual metal ions concentrations were listed in Table 1. The obtained solutions were mixed with the PAAS to make the P/M=25 as well as adding HCl solution and NaOH solution to adjust pH to 7.0. Then the SID-UF experiment was performed to selectively separate metals and the results are shown in Figs. 12 and 13. In the SID-UF experiments, an amount of hyperpure water (pH 7.0) was added to the raw material tank simultaneously to maintain the volume of feed.

The rotating speed was initially controlled at 1,400 rpm to recover the Cu (II). As shown in Fig. 12, the concentration ratios of copper decrease gradually with the progressing feeding, while that of zinc remains constant, indicating the copper has been successfully separated from the electroplating effluent. When the V_m reach to 9.0 L, all of the copper has been recovered. Next, the rotating speed is raised to 2,400 rpm to recover zinc. As a result in Fig. 13, the zinc has been almost collected at V_m=15.0 L. When the zinc is completely separated, the diafiltration experiment is carried out without any water to the feed tank, then the most of water permeate to outside, the regenerated PAAS is obtained ~37 min later, and the recovered efficiency of PAAS is more than 99%. The inadequate recovery of PAAS is possibly caused by the residual of a little amount of shorter PAAS passed through the membrane during the UF experiment. The regenerated PAAS can be reused and the rejections of copper and zinc are 98.4% and 98.7% at the same optimum conditions, respectively. There are thimbleful complexes in the reused PAAS. It can be seen that the complexing ability of regenerated PAAS is excellent. Thus, SID-UF is successful for the selective separation of copper and zinc and the regeneration of PAAS in electroplating effluent.

CONCLUSIONS

The selective separation of copper and zinc and the recovery of polymer were investigated from the laboratory aqueous solution and electroplating effluent using rotating disk membrane by shear induced dissociation coupling with ultrafiltration. The velocity distribution and shear rate distribution were simulated using the CFD software Gambit 2.4 and Fluent 6.3. The results show that shear rate increases with the radius position and the speed, which is similar to Bouzerar et al. The UF tests show that optimal operation conditions for the simultaneous removing both copper and zinc by the PAAS polymer are P/M 25 and pH 7.0. Shear-induced dissociation coupling with ultrafiltration (SID-UF) was used to separate copper and zinc and recover complexant according to the difference of shear stabilities of the two complexes. The order of critical shear rate was PAA-Zn>PAA-Cu at the same pH. The results show that copper and zinc ions can be separated at $1.06\times10^5\ s^{-1}<\gamma<1.58\times10^5\ s^{-1}$ at pH 7.0, and PAAS can also be regenerated at $\gamma>1.58\times10^5\ s^{-1}$ at pH 7.0. Thus, SID-UF can be efficiently used for the separation of metals and the regeneration of complexing agent.

ACKNOWLEDGEMENT

This work was funded by the National Natural Science Foundation of China (Grant NO. 21476265).

REFERENCES

1. M. Al-Shannag, Z. Al-Qodah, K. Bani-Melhem, M. R. Qtaishat and M. Alkasrawi, *Chem. Eng. J.*, **260**, 749 (2015).
2. D. J. Ennigrou, M. Ben Sik Ali and M. Dhahbi, *Desalination*, **343**, 82 (2014).
3. D. Vilela, J. Parmar, Y. Zeng, Y. Zhao and S. Sánchez, *Nano Lett.*, **16**, 2860 (2016).
4. F. Fu and Q. Wang, *J. Environ. Manage.*, **92**, 407 (2011).
5. M. Feizi and M. Jalali, *J. Taiwan Inst. Chem. Eng.*, **54**, 125 (2015).
6. K. R. Desai and Z. V. P. Murthy, *Chem. Eng. J.*, **185**, 187 (2012).
7. J. Song, X. Niu, X. M. Li and T. He, *Process Saf. Environ. Prot.*, **113**, 1 (2018).
8. W. Peng, Z. Xie, G. Cheng, L. Shi and Y. Zhang, *J. Hazard. Mater.*, **294**, 9 (2015).
9. D. Wang, J. Hu, D. Liu, Q. Chen and J. Li, *J. Membr. Sci.*, **524**, 205 (2017).
10. R. Molinari and P. Argurio, *Water Res.*, **109**, 327 (2017).
11. Y. Huang, D. Wu, X. Wang, W. Huang, D. Lawless and X. Feng, *Sep. Purif. Technol.*, **158**, 124 (2016).
12. D. J. Ennigrou, M. Ben Sik Ali, M. Dhahbi and M. Ferid, *Desalin. Water Treat.*, **56**, 2682 (2015).
13. Y. R. Qiu and L. J. Mao, *Desalination*, **329**, 78 (2013).
14. J. Y. Xu, S. Y. Tang and Y. R. Qiu, *J. Cent. South Univ.*, **26**, 577 (2019).
15. J. Zeng, H. Ye and Z. Hu, *J. Hazard. Mater.*, **161**, 1491 (2009).
16. G. Crini, N. Morin-Crini, N. Fatin-Rouge, S. Déon and P. Fievet, *Arab. J. Chem.*, **10**, S3826 (2017).
17. J. Müslehiddinoğlu, Y. Uludağ, H. Ö. Özbelge and L. Yilmaz, *J. Membr. Sci.*, **140**, 251 (1998).
18. K. Kim, J. Y. Jung, J. H. Kwon and J. W. Yang, *J. Membr. Sci.*, **475**, 252 (2015).
19. K. J. Hwang, S. Y. Wang, E. Iritani and N. Katagiri, *J. Taiwan Inst. Chem. Eng.*, **62**, 1 (2015).
20. W. Zhang, N. Grimi, M. Y. Jaffrin and L. Ding, *J. Membr. Sci.*, **489**, 183 (2015).
21. W. Zhang, L. Ding, N. Grimi, M. Y. Jaffrin and B. Tang, *Sep. Purif. Technol.*, **175**, 365 (2017).
22. S. Y. Tang and Y. R. Qiu, *Chem. Eng. Res. Des.*, **136**, 712 (2018).
23. S. Y. Tang and Y. R. Qiu, *Korean J. Chem. Eng.*, **35**, 2078 (2018).
24. J. Gao, Y. Qiu, B. Hou, Q. Zhang and X. Zhang, *Chem. Eng. J.*, **334**, 1878 (2018).
25. L. Chen and Y. Qiu, *Chinese J. Chem. Eng.*, **27**, 519 (2019).
26. K. J. Hwang, S. E. Wu and Y. L. Hsueh, *Sep. Purif. Technol.*, **198**, 16 (2018).
27. R. Bouzerar, M. Y. Jaffrin, L. H. Ding and P. Paullier, *AIChE J.*, **46**, 257 (2000).
28. K. J. Hwang and S. E. Wu, *Chem. Eng. Res. Des.*, **94**, 44 (2015).
29. P. Cañizares, A. Pérez, R. Camarillo and R. Mazarro, *J. Membr. Sci.*, **320**, 520 (2008).
30. Q. Li, L. Chai, Q. Wang, Z. Yang, H. Yan and Y. Wang, *Bioresour. Technol.*, **101**, 3796 (2010).
31. C. Belle, C. Beguin, I. Gautier-Luneau, S. Hamman, C. Philouze, J. L. Pierre, F. Thomas, S. Torelli, E. Saint-Aman and M. Bonin, *Inorg. Chem.*, **41**, 479 (2002).
32. A. Mendoza, J. Aguilar, M. G. Basallote, L. Gil, J. C. Hernández, M. A. Máñez, E. García-España, L. Ruiz-Ramírez, C. Soriano and B. Verdejo, *Chem. Commun.*, **3**, 3032 (2003).
33. M. Y. Jaffrin, *J. Membr. Sci.*, **324**, 7 (2008).
34. F. Ellouze, B. Seantier, N. Ben Amar and A. Deratani, *Sep. Purif. Technol.*, **204**, 226 (2018).
35. L. E. Eary and D. Rai, *Environ. Sci. Technol.*, **22**, 972 (1988).
36. C. E. Barrera-Díaz, V. Lugo-Lugo and B. Bilyeu, *J. Hazard. Mater.*, **223**, 1 (2012).